Yu et al. BMC Medicine (2025) 23:261
https://doi.org/10.1186/s12916-025-04089-9

BMC Medicine

RESEARCH

Open Access

Molecular mechanisms explaining sex-specific functional connectivity changes in chronic insomnia disorder

Liyong Yu[1†], Zhifu Shen[2,3†], Wei Wei[1], Zeyang Dou[1], Yucai Luo[1], Daijie Hu[1], Wenting Lin[4], Guangli Zhao[4], Xiaojuan Hong[1] and Siyi Yu[1*]

Abstract

Background This study investigates the hypothesis that chronic insomnia disorder (CID) is characterized by sex-specific changes in resting-state functional connectivity (rsFC), with certain molecular mechanisms potentially influencing CID's pathophysiology by altering rsFC in relevant networks.

Methods Utilizing a resting-state functional magnetic resonance imaging (fMRI) dataset of 395 participants, including 199 CID patients and 196 healthy controls, we examined sex-specific rsFC effects, particularly in the default mode network (DMN) and five insomnia-genetically vulnerable regions of interest (ROIs). By integrating gene expression data from the Allen Human Brain Atlas, we identified genes linked to these sex-specific rsFC alterations and conducted enrichment analysis to uncover underlying molecular mechanisms. Additionally, we simulated the impact of sex differences in rsFC with different sex compositions in our dataset and employed machine learning classifiers to distinguish CID from healthy controls based on sex-specific rsFC data.

Results We identified both shared and sex-specific rsFC changes in the DMN and the five genetically vulnerable ROIs, with gene expression variations associated with these sex-specific connectivity differences. Enrichment analysis highlighted genes involved in synaptic signaling, ion channels, and immune function as potential contributors to CID pathophysiology through their influence on connectivity. Furthermore, our findings demonstrate that different sex compositions significantly affect study outcomes and higher diagnostic performance in sex-specific rsFC data than combined sex.

Conclusions This study uncovered both shared and sex-specific connectivity alterations in CID, providing molecular insights into its pathophysiology and suggesting considering sex differences in future fMRI-based diagnostic and treatment strategies.

Keywords Chronic insomnia, Functional connectivity, Default mode network, Sex-specific effects, Transcriptional signatures, Machine learning

[†]Liyong Yu and Zhifu Shen contributed equally to this work.

*Correspondence:
Siyi Yu
cdutcmsy@gmail.com
Full list of author information is available at the end of the article

Background

Chronic insomnia disorder (CID) is a complex condition with diverse manifestations and unclear links to its biological foundations. Meta-analysis revealed that women are at a risk ratio of 1.4 compared to men, as likely to experience CID [1], indicating female sex as a risk factor, though the exact reasons for sex differences in CID remain elusive. There are subtle yet significant sex-based variations in CID's impact on brain structure and function [2, 3], as well as symptom types. For instance, anxiety and depression, which frequently accompany insomnia, tend to be more prevalent in women than in their male counterparts [4, 5]. Previous research [6] has also uncovered sex-specific genetic expression related to insomnia, suggesting that different biological processes may influence the disorder in men and women.

Resting-state functional magnetic resonance imaging (rsfMRI) is essential for understanding the neurobiology of CID. Studies have found alterations in resting state functional connectivity (rsFC) within the default mode network (DMN), subcortical areas, and other CID-related networks [7–13], which have potential utility as transdiagnostic markers and biomarkers of remission [14, 15]. One of the consistent findings in CID-related fMRI research is the altered connectivity in the DMN [16, 17], a pattern also observed in various neuropsychiatric disorders such as autism [18], depression [19], and schizophrenia [20]. This altered connectivity in the DMN is associated with issues like conflict control and anxiety [7, 21] and could be a target for interventions like neurostimulation [22] and biofeedback [23]. Other studies have identified divergent interactions between the DMN and executive-control network, which may contribute to daytime cognitive dysfunction [12, 24]. However, the research on DMN connectivity in CID presents mixed results, with some studies indicating decreased rsFC [25–27]; others have not [28, 29], and there is no large-scale analysis of rsFC in this network. Surprisingly, relatively limited studies to date have tested for sex-specific effects on rsFC in CID [30], due in part to power constraints. Whether CID is associated with distinct rsFC patterns in women versus men remains unclear.

The underlying molecular mechanisms leading to rsFC changes in CID also remain unclear. Genome-wide association studies with over 100,000 participants have identified many genetic risk variants for CID, highlighting a highly polygenic inheritance pattern where each variant contributes minimally to the overall risk [6, 31, 32]. The complex interplay of these numerous genetic factors in CID's pathophysiology is not yet clear. Emerging evidence suggests that spatial variations in brain gene expression might influence rsFC [33, 34]. For example, studies have shown that regional differences in gene expression could be linked to the distribution of morphometric and connectivity changes in neuropsychiatric conditions like depression [35, 36] and schizophrenia [37, 38]. However, it is still uncertain whether these regional gene expression differences can specifically explain the rsFC changes within the specific connections and networks observed in CID. Additionally, whether these genetic correlates of rsFC in CID vary between sexes remains unclear.

In our study, we sought to examine the hypothesis that (1) CID is linked to sex-specific patterns of abnormal connectivity and (2) specific molecular mechanisms could influence CID pathophysiology by modulating functional connectivity. Utilizing a substantial rsfMRI dataset comprising 395 individuals, including both CID patients and healthy controls, we initially explored whether CID is associated with sex-specific rsFC effects. Our focus was on the DMN, known to be implicated in fMRI studies [16, 39, 40] of insomnia, and five regions of interest showing genetic vulnerability in CID [41]. Additionally, using microarray data from the Allen Human Brain Atlas (AHBA) [42], we investigated whether certain molecular mechanisms could potentially affect CID pathophysiology by altering functional connectivity in relevant networks. Furthermore, to assess how these observed sex differences impact future research, we investigated the effect of sex differences in rsFC with different sex compositions and utilized machine learning classifiers to distinguish CID from healthy controls based on sex-specific rsFC data.

Methods

Recruitment and assessment

The diagnosis of CID was conducted through structured interviews by five neurologists with 8–15 years of psychiatric experience, based on the Diagnostic and Statistical Manual of Mental Disorders, Fifth Edition (DSM-V) and the International Classification of Sleep Disorders, Third Edition (ICSD-3) [43]. Inclusion and exclusion criteria were detailed in Supplementary Methods (Additional file 1: Methods S1 [43, 44]). All participants were aware of the study's purpose and provided informed written consent. Twelve healthy subjects and 21 patients with CID were excluded because of excessive head movement (see fMRI preprocessing for exclusion criteria), leaving 199 CID patients and 196 healthy controls (HCs) available for analyses. Clinical and demographic characteristics of CID and HCs are summarized in Table 1.

Neuroimaging data acquisition

T1w and rs-fMRI images were acquired using a GE 3.0 T MRI scanner (Discovery MR750; GE Healthcare, Milwaukee, WI, USA). The following settings were used to acquire sagittal 3D T1-weighted images: repetition time

Table 1 Demographic and clinical characteristics of CID and healthy controls

Characteristics	CID Male ($n=67$)		CID Female ($n=132$)		HC Male ($n=76$)		HC Female ($n=120$)		Diagnosis		Sex		Diagnosis* Sex	
	Mean	SD	Mean	SD	Mean	SD	Mean	SD	F	*p*	F/t	*p*	F	*p*
Age (years)	36.33	11.34	35.44	11.81	38.01	12.37	34.30	12.83	0.00	0.99	3.35	0.07	1.23	0.27
Education (years)	14.24	3.38	14.77	3.20	15.11	2.88	15.12	3.72	2.44	0.12	0.56	0.45	0.54	0.46
Mean FD (mm)	0.10	0.04	0.09	0.03	0.10	0.07	0.09	0.05	0.73	0.39	1.65	0.20	0.06	0.80
Mean DVARS	0.95	0.26	0.90	0.26	0.93	0.29	0.93	0.29	0.09	0.76	0.83	0.36	0.70	0.40
PSQI	13.76	2.70	13.20	2.72	3.11	1.45	3.20	1.47	2169	0.00*	0.95	0.32	2.03	0.16
ISI	17.75	4.09	17.16	4.15	2.82	2.23	2.64	2.40	1875	0.00*	1.14	0.29	0.34	0.56

DVARS, temporal derivative of time courses of RMS variance over voxels

Abbreviations: *FD* Framewise displacement, *CID* Chronic insomnia disorder, *HCs* Healthy controls, *PSQI* Pittsburgh sleep quality index, *ISI* Insomnia severity index

*indicates $p<0.0001$

(TR) = 7.06 ms; echo time (TE) = 3.04 ms; flip angle (FA) = 12°; acquisition matrix = 256 × 256; slice thickness = 1 mm, no gap; and 188 sagittal slices. The rs-fMRI images were obtained with the following parameters: TR = 1700 ms, TE = 30 ms, FA = 90°, acquisition matrix = 64 × 64, voxel size = 3.75 × 3.75 × 3.2 mm^3, thickness = 3.5 mm, and number of slices = 33.

MRI data preprocessing

The preprocessing of T1w and rs-fMRI data was performed on fMRIPrep 22.1.1 pipelines [45]. For the T1w image, a sequence of procedures was conducted, which encompassed intensity non-uniformity correction, skull-stripping, tissue segmentation, and spatial normalization to a standard space through nonlinear registration. The fMRI preprocessing procedures encompassed reference volume generation, head-motion parameter estimation prior to spatiotemporal filtering, slice-time correction, co-registration with the T1w reference, extraction of confounding time-series, and resampling into standard space. During the above processes, framewise displacement (FD) and the standard temporal derivative of time courses of RMS variance over voxels (DVARS) were calculated across the entire time point for each subject as head movement measurements. Additionally, fMRIPrep was used to estimate 36 confounds from the preprocessed time points [46, 47]. These confounding matrices were utilized within xcp_d 0.0.4 [47, 48] to mitigate motion-related artifacts and noise in rsfMRI data. Processed functional time series were then extracted from 360 cortical areas defined by an extensively validated functional parcellation [49] and 19 subcortical regions [50]. In cases of partial coverage for each parcel, uncovered voxels (values of all zeros or NaNs) were either ignored (when the parcel had > 50.0% coverage) or were set to zero (when the parcel had < 50.0% coverage). Then pairwise functional connectivity was computed, operationalized as Pearson's correlation of unsmoothed time series from each parcel. Subjects were excluded if they had more than 20% time point with 0.5 mm movement based on FD and/or 1.5 standard DVARS. Twelve healthy subjects and 21 patients with CID were excluded because of excessive head movement. See "Additional file 1: Methods S2 [45–54]" for more details.

Effects of CID and sex on rsFC in the DMN and five genetically vulnerable regions of interest

Leveraging preprocessed time-series data from blood oxygen level-dependent signals, we generated rsFC matrices delineating the connectivity between 83 regions of interest (ROIs) (Additional file 1: Table S1) within the DMN and its interactions with the other brain regions. A two-way factorial analysis of variance (ANOVA) was employed to delineate the impacts of CID diagnosis and the interactions between sex and CID on the rsFC matrix attributes. Post hoc *t*-tests were subsequently conducted to pinpoint significant rsFC alterations in male and female subjects diagnosed with CID compared to their respective HC groups. We also calculated shared effects across sexes by summarizing post hoc *t*-values in brain regions that showed statistical significance in both male and female groups. These shared effects highlight a subset of regions with a consistent CID impact across sexes. The threshold for statistical significance was set at $p < 0.05$, adjusted for the False Discovery Rate (FDR) correction to control type I error ($n = 379$ comparisons).

Additionally, we used a two-way ANOVA to test for the main effects of CID diagnosis and sex-by-CID interactions on rsFC seeded from each of five ROIs that exhibited abnormal gene expression signatures in a previous study [41]. These regions included the dorsolateral prefrontal cortex (DLPFC; Brodmann Area [BA] 9), anterior cingulate cortex (ACC; BA24), nucleus accumbens (NAc), caudate nucleus (CNs), and putamen. Similar

post hoc *t*-tests were employed to uncover significant rsFC changes in patients with CID compared to their respective HC groups. A significant level was set at $p_{FDR} < 0.05$. Venn diagrams served to illustrate the rsFC modifications distinctly observed in males and females with insomnia, as well as those shared by both groups. Additionally, we assessed if the quantity of sex-specific rsFC changes exceeded the levels predicted by random chance. This was conducted by contrasting the observed number against the random permutation of sex labels within the dataset.

Decoding rsFC changes from a molecular perspective

This study initially delineated normative gene expression patterns from the AHBA [42], and mapped these profiles onto the Glasser functional parcellation [49]. Subsequently, partial least squares regression (PLS-R) [55] was employed to discern the covariance between gene expression patterns and alterations in sex-specific connectivity. This PLS-R analysis was conducted separately for male and female participants within the five specific ROIs (DLPFC, ACC, NAc, CNs, and putamen) to capture associated gene expression. Furthermore, to interpret PLS-R results, we used gene-category enrichment analyses [56] to understand which molecular pathways were enriched among the most highly associated genes.

Estimation of microarray gene expression maps

The AHBA gene expression data [42] was processed utilizing the abagen toolbox (version 0.1.3; https://github.com/rmarkello/abagen) [57], incorporating steps such as filtering of microarray probes based on intensity, selection of a single probe per gene, matching of samples to brain regions as defined by the functional parcellation [49], normalization, and aggregation of data both within and across parcellations. The final gene expression data was represented by a 360 × 15,633 matrix for each donor, relating brain regions to the retained genes. Additionally, genes with low similarity across donors ($r < 0.2$) were removed, resulting in a total of 12,506 genes. As the right hemisphere data was only available for two participants, the transcriptomic-imaging association analysis was limited to the left hemisphere's cortical areas [37], represented by a 180-region × 12,506-gene matrix.

Identifying gene expression data correlated with sex-specific rsFC changes

PLS-R was applied to explore the relationship between changes in regional connectivity and gene expression patterns [37]. Distinct PLS-R models were developed for both sexes across five genetically vulnerable ROIs: DLPFC, ACC, NAc, CNs, and putamen. A total of ten models (5 ROIs × 2 genders) were generated. Each model utilized a predictor matrix (180 × 12,506) comprising AHBA's regional gene expression data against a response vector of 180 elements representing the magnitude of CID-associated connectivity alterations in the left cortical area, originating from one of the five ROIs for each sex. The PLS1 represented a linear composite of gene expression scores, weighted to reflect their collective covariance with alterations in regional connectivity most closely. This component is designed to capture the maximal covariance between the gene expression (predictor) and the connectivity changes (response), although it does not exclusively focus on the variance within the response variable alone. The following analysis concentrated primarily on PLS1 [37]. To ascertain the robustness and significance of each gene's contribution within the PLS1, a bootstrapping technique was employed, involving 10,000 resampling iterations across the 180 brain regions. This procedure enabled the calculation of *Z*-scores for each gene, based on the ratio of its PLS1 loading to the bootstrap standard error, thereby facilitating a ranked assessment of gene contributions to the PLS1 [37]. The analytical code for this process was adapted from a publicly available resource on GitHub provided by Sarah Morgan [37], available at https://github.com/SarahMorgan/Morphometric_Similarity_SZ.

Statistical testing of PLS components

To validate the statistical significance of the gene-neuroimaging correlations revealed by the PLS models, we compared the real-data-derived PSL1 against null distributions. These distributions were generated from 10,000 spatial permutations (the "spin test"). This permutation involved randomly rotating the neuroimaging vector rows based on a spherical projection of the cortical surface [58]. The spatial permutation technique is available at https://github.com/frantisekvasa/rotate_parcellation. This method ensures the preservation of the inherent correlational structure of the cortical surface data, offering stringent control against false positives in contrast to conventional random permutation tests [58]. Additionally, a simpler null model was conducted by randomly shuffling all 180 ROIs within the response vectors across 10,000 iterations. This process was repeated for each of the five predetermined ROIs across both male and female groups, yielding ten distinct null models. These models facilitated the examination of null PLS1 variance against the actual PLS1 variance derived from original data, focusing on each ROI-specific model per sex. A PLS1 explained variance exceeding the 95 th percentile in the distribution of the explained variance from both the spatially rotated (p_{spin}) and the randomly permuted (p_{rand}) null models was considered statistically significant. Significance levels were adjusted for multiple comparisons

across the ten PLS-R models (5 ROIs ×2 sexes) using FDR correction.

Reproducibility testing of PLS1

To evaluate the reproducibility of the gene-neuroimaging correlations revealed by the above ten PLS-R models, we conducted ten rounds of ten-fold cross-validation for each module. Each model was trained on a randomly selected 90% subset of subjects, maintaining a consistent proportion of CID cases in both the training (90%) and testing (10%) groups. Then we separately used two sample *t*-tests to calculate the rsFC effect as a response variable for the training and testing sets. The 10% subset of subjects' impact of CID on rsFC previously held out of the training process was then applied to predict the training sample. The predictive ability of held-out data was quantified using the Pearson correlation coefficient (r_{ho}), calculated as follows:

$$r_{ho} = \mathrm{Corr}\left(\mathrm{X}^{*}\mathrm{Y}_{\mathrm{train}}, \mathrm{Y}_{\mathrm{test}}\right)$$

Here, r_{ho} denotes the Pearson correlation coefficient in the held-out data, with $\mathrm{Y}_{\mathrm{train}}$ representing the response vectors from the training subset, X is the gene predictor matrix, and $\mathrm{Y}_{\mathrm{test}}$ is the response vectors from the held-out subset. The expression $\mathrm{X}^{*}\mathrm{Y}_{\mathrm{train}}$ is the PLS1 loading weights trained on 90% of the data using PLS-R. This process was iterated 100 times—across ten cycles of ten-fold cross-validation—employing different randomly chosen 10% subsets for each repetition to ensure robust validation across multiple data splits. Further, to evaluate the statistical significance of the predictive ability in held-out data, the diagnostic labels for CID were randomly permuted, and null permutation testing for r_{ho} was conducted over the same 100 iterations. The average r_{ho} values from the genuine and permuted data across ten-fold cross-validations were compared using a corrected resampled *t*-test [59], then a *p*-value representing significance for the r_{ho} in a PLS-R module was calculated. The above process resulted in 10 reproducible *p*-values for a total of ten PLS-R modules across 5 ROIs ×2 sexes. Those 10 *p*-values were then used for FDR correction, with a significant level at $p_{\mathrm{FDR}} < 0.05$.

Gene category enrichment analysis

For statistically significant PLS models, the resulting ranked gene lists (*Z*-score >3 or < − 3, $p_{\mathrm{FDR}} < 0.05$) [37, 60] were tested for overrepresentation of gene ontology (GO) terms using the gene category enrichment analysis tool (available at https://github.com/benfulcher/GeneCategoryEnrichmentAnalysis; according to Fulcher et al. [56]). Biological process categories are associated with specific subsets of genes as annotated in the Gene Ontology (geneontology.org). For each significant PLS model, the score for an enriched category was calculated as the mean gene *Z*-score in the bootstrapping procedure within the category. A null model was created by permuting the response variable 10,000 times, ensuring the maintenance of spatial autocorrelation using the previously described spin test. Following this, PLS analysis was reapplied to the original gene expression matrix and the permuted response variables, allowing for the recalculation of null genes and enriching the null GO category biological process. The significance *p*-value (p_{spin}) for each GO category was calculated based on its occurrence frequency relative to the permuting number. A significant level was set at $p_{\mathrm{spin}} < 0.05$.

Additionally, we performed an overlap analysis of the significant genes (*Z*-score >3 or < − 3, $p_{\mathrm{FDR}} < 0.05$) identified across all significant and reproducible PLS-R models to delineate the shared gene expression profiles associated with sex-specific connectivity changes. Furthermore, to comprehensively elucidate the relationship between gene expression and connectivity alterations, we conducted a multi-gene list meta-analysis. This analysis integrated risk genes from a genome-wide association study (GWAS) on insomnia [41] with the significant gene lists (*Z*-score >3 or < − 3, $p_{\mathrm{FDR}} < 0.05$) derived from the significant PLS-R models. The meta-analysis for each PLS model was performed separately using the Metascape platform [61] (https://metascape.org/gp/index.html#/main/step1).

Simulating the impact of sex differences in rsFC

To elucidate the effect of sex compositions on CID-related rsFC outcomes and the development of fMRI biomarkers, two analyses were conducted. Firstly, we assess the potential influence of sex-based effects by simulating 1000 studies with different sex compositions. These simulations explored the CID effect on rsFC using subsets of our dataset with varied sex compositions, spanning from entirely CID to entirely HC cohorts. Specifically, each simulation involved a subset of 60 individuals with CID and 70 HCs, stratified into one of seven distinct sex ratios (0%, 20%, 33%, 50%, 67%, 80%, and 100% female), uniformly applied across both CID and HC groups. Within every iteration of these subsets, a linear regression model was employed to assess the effect of CID on the mean of all rsFC features connecting the 83 DMN regions, with age included as a covariate. The significance level was set at $p_{\mathrm{FDR}} < 0.05$ ($n = 379$ comparisons).

Secondly, elastic-net regularized general linear models (EN-GLMs) were trained to predict CID status using male-only, female-only, and combined-sex rsFC data, and we compared the performance of those models. For each model category (male, female, combined-sex), 94

subjects were randomly chosen for model training, with an independent testing set of 47 subjects from the same category selected for validation, aiming to assess the predictive performance of each EN-GLM. This process was replicated 100 times, facilitating the calculation of average performance metrics, specifically the area under the receiver operating characteristic curve (AUC), for models across all three groups. For every iteration, the 47 subjects designated for testing were exclusively reserved for model evaluation, ensuring no overlap with the training phase. The means for each rsFC in 379 regions across cortical and subcortical areas connecting the 83 DMN regions were selected as features to train EN-GLM. The EN-GLMs incorporated an alpha parameter set to 0.5 to balance ridge and lasso penalization equally. Utilizing MATLAB's "lassoglm" function, which cycles through 80 lambda values, the models were optimized across a variable feature set, ranging in size from 1 to 379 features. The beta-weights for each feature, derived over the course of 100 modeling iterations, were averaged to calculate the absolute loading weight as an index of feature importance in classification. This average absolute loading weight was visually represented on a brain map, illustrating the anatomical distribution of features significant for predicting CID status across the male, female, and mixed-sex EN-GLMs.

Results

Shared and sex-specific effects associated with the DMN

Our analysis uncovered broad main effects of CID, particularly pronounced effects were observed in the anterior/posterior cingulate cortex, dorsomedial prefrontal cortex, and insula (Fig. 1a), corroborating findings from prior neuroimaging meta-analyses of insomnia [16]. Additionally, we identified significant main effects associated with sex (Fig. 1b) and interactions between sex and CID that have not been thoroughly explored in prior research [62], and those interaction effects were mainly observed in extensive regions of the ventromedial prefrontal cortex, posterior cingulate cortex, and the medial temporal cortex (Fig. 1c). Subsequent post hoc analysis unveiled a few shared effects across sexes (Fig. 1d; Additional file 1: Fig. S1), such as diminished connectivity in the ventromedial prefrontal cortex, alongside numerous sex-specific effects. Notably, sex-specific hypoconnectivity within the DMN was predominantly observed in males, particularly in the posterior cingulate cortex and ventromedial prefrontal cortex (Fig. 1e; Additional file 1: Table S2). In contrast, females with CID showed decreased sex-specific rsFC in the medial temporal cortex (Fig. 1f; Additional file 1: Table S3). Additionally, we conducted post hoc analyses in other regions to explore sex-distinct effects, where no significant interactions were found. We observed that females with CID exhibited increased sex-distinct rsFC in regions such as the superior parietal cortex, medial cingulate cortex, and visual cortex, while males with CID exhibited decreased sex-distinct rsFC primarily in the dorsomedial prefrontal cortex (Fig. 1e, f).

To delve deeper into the relationship between CID status, sex, and connectivity within the DMN, we analyzed and visualized the outcomes of post hoc *t*-tests examining the impact of CID across sexes and the influence of sex within the HCs group (Fig. 2a–c). It was noted that connectivity within the DMN was predominantly reduced among males diagnosed with CID (Fig. 2a) and within healthy females (Fig. 2b) when each was compared to healthy males without a CID diagnosis. Given the significant age difference between male (M = 38.01, SD = 12.37) and female HCs (M = 34.30, SD = 12.83; t (194) = 2.00, p = 0.047), we applied a post hoc linear regression model, adjusting for age, to confirm reduced DMN connectivity in healthy males compared to females. Supplementary analyses further corroborated this finding (Additional file 1: Fig. S2). The observed relative augmentation in CID's impact on DMN connectivity among females (Fig. 2c) can be attributed to an already existing reduction in DMN connectivity in healthy females when contrasted with their male counterparts. These observations were consistent across several DMN sub-regions, including the anterior sections (inferior frontal cortex, dorsolateral prefrontal cortex, and anterior cingulate cortex) as well as the lateral portions (inferior parietal cortex).

Shared and sex-specific effects in five genetically vulnerable ROIs

We identified shared and sex-specific effects of CID on rsFC across all five ROIs (Fig. 3a; Additional file 1: Fig. S3). Instances of sex-specific impacts were notably more prevalent than effects common to both sexes in all five ROIs, with many of these effects markedly divergent between men and women, occasionally in opposite directions (Fig. 3b–d). Women generally exhibited increased connectivity, whereas men displayed reduced connectivity. For example, in the DLPFC, the influence of CID on rsFC showed stark contrasts between sexes. Men with CID experienced diminished connectivity to several areas, including the medial prefrontal, temporal pole, and medial cingulate cortex (Fig. 3d), a pattern not seen in women (Fig. 3b). In other regions such as the nucleus accumbens, anterior cingulate cortex, caudate nucleus, and putamen, the majority of effects were unique to one sex, with a minor proportion (ranging from 5.5 to 8.0%) being shared between men and women (Fig. 3e). To assess if the incidence

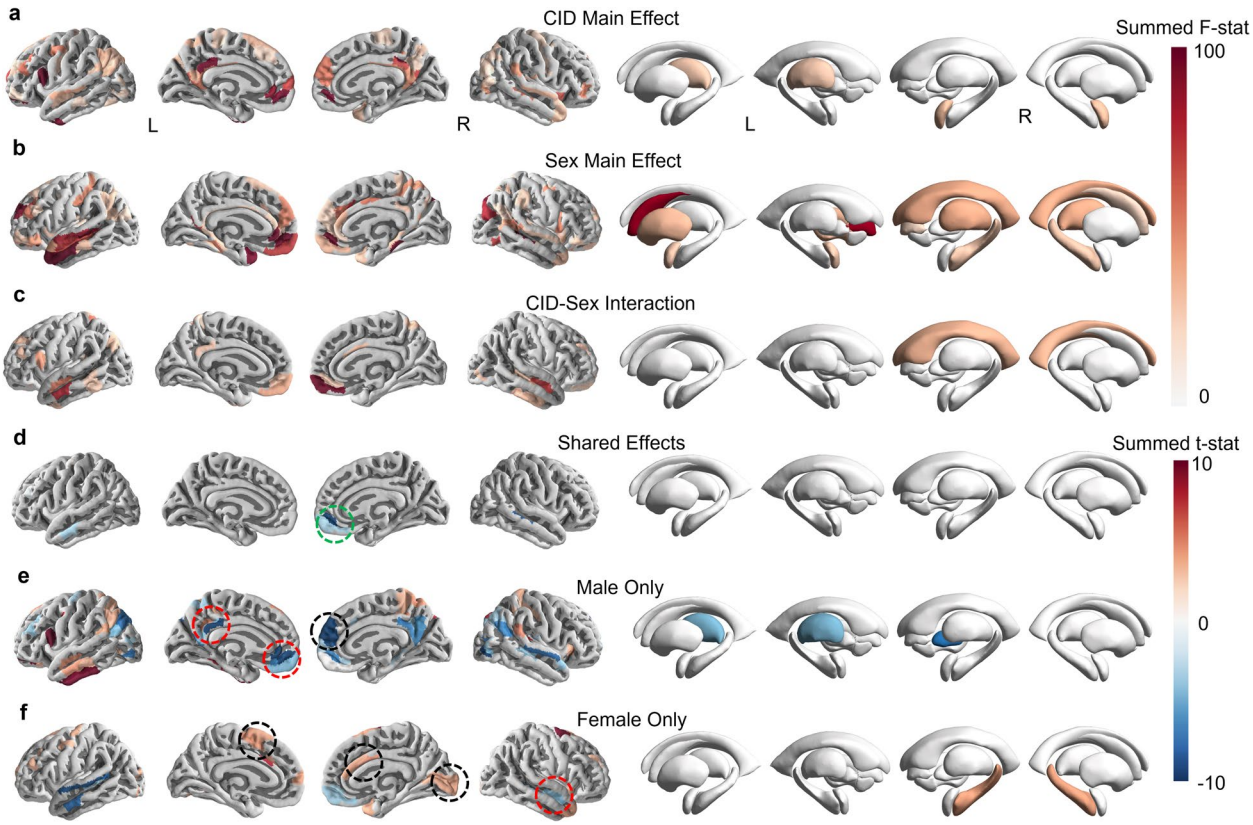

Fig. 1 Shared and sex-specific rsFC effects associated with the DMN. **a**–**c** Color maps illustrate the distribution of significant F-statistics ($p_{FDR} < 0.05$) from a 2-way ANOVA, by analyzing rsFC effects for each parcel connecting 83 DMN regions of interest. The overall significant CID main effects (**a**), sex main effects (**b**), and CID-by-sex interaction effects (**c**) are summarized for each functional parcel by summing 83 DMN nodes. **d**–**f** Summarize post hoc *t*-values in CID-sex interaction effect for neuroanatomical visualization, separately plotting rsFC changes in male (**d**), female (**e**), and both sexes (**f**), similar to the summation approach in **a**, **b,** and **c**. Aggregating results by grouping Glasser parcels into relevant networks can be found in Additional file 1: Fig. S1. Annotations with red dashed circles indicate sex-specific DMN-associated alterations, black dashed circles indicate sex-distinct DMN-associated alterations, and green dashed circles mark shared connectivity changes, as discussed in the main text. Abbreviations: DMN, default mode network; CID, chronic insomnia disorder; HC, healthy controls; rsFC, resting-state functional connectivity; L, left; R, Right

of sex-specific effects exceeded what might be anticipated by random chance, we evaluated the prevalence of these effects against outcomes from datasets with sex labels permuted randomly. This analysis confirmed the presence of significant sex-specific effects in two out of the five examined regions (Fig. 3f).

Transcriptional signatures underlying sex-specific rsFC effects

PLS-R was applied to uncover gene clusters whose expression patterns closely aligned with the spatial variations in connectivity alterations linked to CID within five key ROIs (Fig. 4a). To verify the consistency and reproducibility of the gene-connectivity relationships identified by PLS-R, we conducted a ten times ten-fold cross-validation to assess the predictive ability in independent testing data. This approach demonstrated that gene expression exhibited a spatial congruence with connectivity alterations most consistently and reproducibly across three ROIs (Fig. 4b–e) in the independent testing data: the DLPFC for both males and females, the putamen for females only, and the NAc for males only. While the primary focus was on the most reproducible findings across these regions, significant gene-connectivity correlation was also found across all ten models assessed by both a spatial permutation test and a traditional permutation test that employs random data shuffling (Additional file 1: Fig. S4).

To elucidate how different gene sets contributed to the connectivity deviations observed in specific ROIs among CID-affected males and females, we prioritized the genes within each model. This was achieved by organizing the 12,506 genes according to their PLS loading weights, which reflect their importance in predicting the connectivity changes originating from each ROI. Genes with the highest positive loading weights, indicative of increased expression in cortical areas linked to

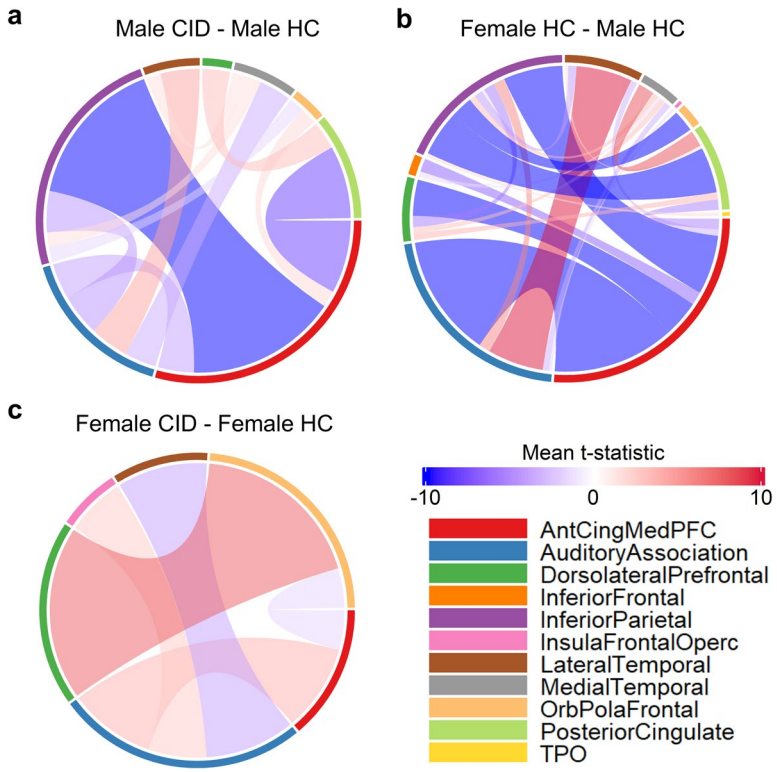

Fig. 2 Sex-specific rsFC effects within DMN. Circle plots (**a**–**c**) display rsFC in eleven DMN subregions, with colors and band width reflecting average significant t-statistics ($p_{FDR} < 0.05$). Warm colors indicate heightened connectivity in CID patients vs. HCs (**a, c**) or healthy females vs. healthy males (**b**). Abbreviations: DMN, default mode network; CID, chronic insomnia disorder; HC, healthy controls; Insula_FrontalOperc, Insular_and_Frontal_Opercular; AntCing_MedPFC, Anterior_Cingulate_and_Medial_Prefrontal; OrbPolaFrontal, Orbital_and_Polar_Frontal

heightened connectivity in CID, are illustrated in Fig. 4f. Our results revealed two key observations. Firstly, among females, genes with prominent positive loading weights in the CNs model also demonstrated positive weights in the putamen model, whereas in the DLPFC model, these genes typically exhibited negative weights. Secondly, the genes in the DLPFC model displayed a tendency to differ between sexes, with genes having the highest positive loading weights in women showing lower weights for the same ROI in men, and vice versa. This trend was also apparent among genes with the most significant negative loading weights, represented in Fig. 4g, which corresponded to high expression in regions associated with reduced connectivity in CID. Quantitative validation of these observations confirmed that such patterns were consistent beyond just the top-ranked genes of each model, as evidenced by correlation tests between the PLS1 loading weight vectors for each model, detailed in Fig. 4h.

Subsequently, gene-category enrichment analysis was employed to determine if the significant genes (Z-score >3 or <-3, $p_{FDR} < 0.05$) in the four prior significant and reproducible models were indicative of particular biological processes. Through enrichment analysis, it was revealed that genes exhibiting the highest positive or negative loading weights significantly and predominantly corresponded to pathways involved in synaptic function, ion channels, and immune signaling (Fig. 5; Additional file 1: Fig. S5). Three genes—ZDHHC2, VAT1L, and CHST1—were consistently found across all models (Additional file 1: Fig. S6). Additionally, our results revealed that the GWAS gene list and the gene lists from the PLS models (PLS1 +and PLS1 −) share additional GO biological processes, particularly those related to brain development and behavior (Additional file 1: Fig. S7).

Sex-specific rsFC effects on biomarker development

To assess the impact of sex differences in rsFC on research outcomes, we analyzed DMN connectivity variations across 1000 bootstrapped datasets (comprising 60 CID patients and 70 healthy controls) for a spectrum of gender ratios, from all-male to all-female cohorts. Our results revealed that the results varied obviously with sex composition (Fig. 6a, b). Predominantly, an increase in female proportion within the simulated

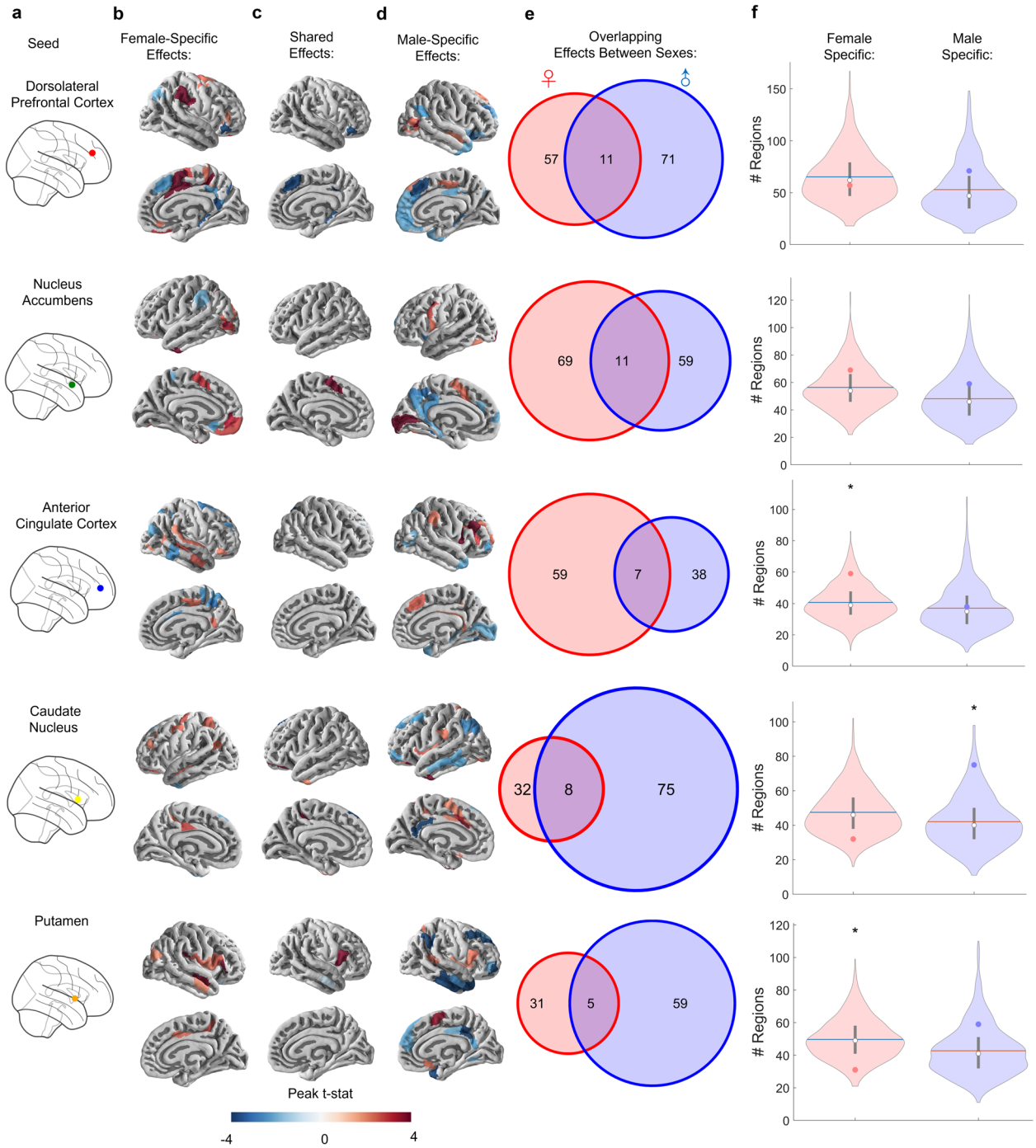

Fig. 3 Sex-specific effects in five genetically vulnerable regions of interest (**a**). **b**–**d** Color maps illustrating CID versus healthy control *t*-statistics, showing rsFC effects that are female-specific (**b**), common to both genders (**c**), and male-specific (**d**) across five ROIs. Each row labels a seed, showing peak *t*-statistics for functional parcels across both hemispheres. Parcels showing significant main effects ($p_{FDR} < 0.05$) of CID, sex, or their interaction are detailed in Fig. S3. **e** Venn diagrams quantify sex-specific versus shared connectivity effects, with a significant threshold ($p_{FDR} < 0.05$) for each seed. **f** Boxplots visualize the female- (left) and male-specific (right) connectivity effects in a null model, generated by randomly permuting sex labels 1000 times. Empirical counts of sex-specific effects from (**e**) are marked with red and blue dots. * indicates $p < 0.05$

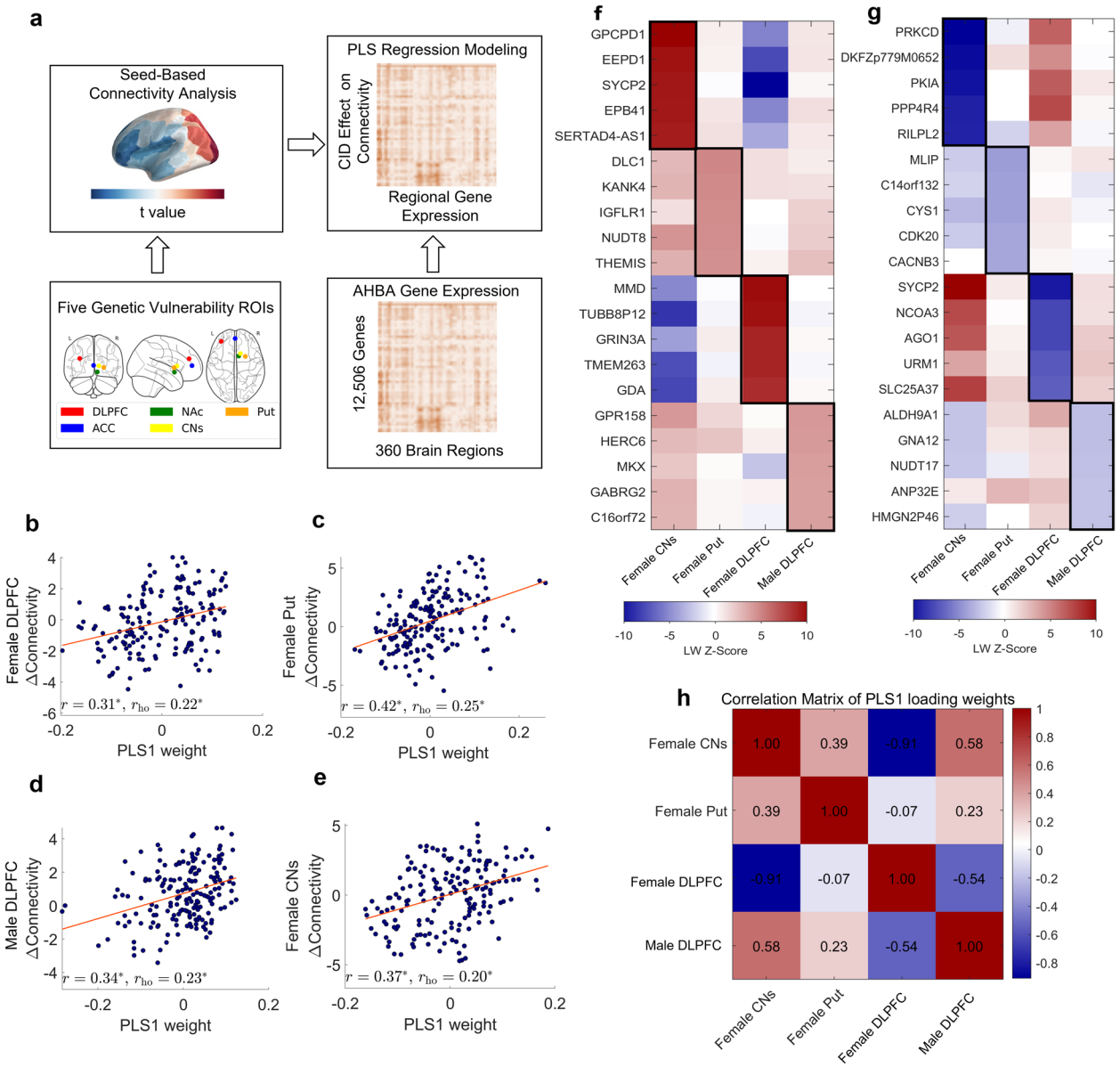

Fig. 4 Transcriptional signatures underlying sex-specific rsFC effects. **a** Diagram illustrating PLS-R analysis to explore spatial associations between regional gene expression and rsFC changes across five genetically vulnerable ROIs (DLPFC, NAc, ACC, CNs, and Put). **b**–**e** Scatterplots from PLS-R revealing significant and reproducible correlations between gene expression and rsFC changes in specific models: DLPFC in females (**b**), Put in females (**c**), DLPFC in males (**d**), and CNs in females (**e**). Each point indicates a brain region's PLS1 loading weight against its rsFC effect. Displayed below are the PLS1 correlation coefficient (*r*) and average correlation (r_{ho}) from 10 rounds of tenfold cross-validation, with significance tested via spin test + FDR correction. * indicates $p_{FDR} < 0.05$. **f**, **g** Heatmaps depicting the LW *Z*-scores for the top 5 genes (in rows) with the strongest positive LWs (**f**) and the strongest negative LWs (**g**) in the PLS models depicted in (**b**–**e**), shown in columns. **h** Spearman correlation of PLS1 loading weights in four PLS models from **b**–**e**. Abbreviations: PLS, partial least squares; PLS1, the first PLS component; LW, loading weight; DLPFD, dorsolateral prefrontal cortex; ACC, anterior cingulate cortex; NAc, nucleus accumbens; CNs, caudate nucleus; Put, putamen

subsets correlated with a notable rise in hyperconnectivity findings within the DMN (Fig. 6a). For example, comparisons between samples comprising 50% and 67% female participants—a demographic distribution frequently observed in existing neuroimaging research [16, 63] on insomnia—demonstrated significant disparities in outcomes. Specifically, samples with 67% female composition showed a significant increase in regions of hyperconnectivity within the DMN compared to those with 50% female composition (Fig. 6b).

Furthermore, we assessed whether the sex-specific rsFC could notably affect the performance of fMRI-based diagnostic biomarkers. This involved training EN-GLM to classify CID status from rsFC patterns (Fig. 6c), using data from each sex separately as well as combined, with performance validation on an independent testing set. Results indicated that EN-GLMs tailored to each sex outperformed the generalized model trained on the combined sex dataset, achieving consistently higher performance (Fig. 6d, e). To identify which rsFC features were reliable in predicting CID status, we computed the average absolute loading weight for each connectivity feature across 100 iterations of the model. Consistent with our earlier findings, there was a noticeable variation in predictive features between sexes: the ventromedial prefrontal cortex, medial cingulate cortex, and superior parietal cortex were prominent in models for males, while the anterior cingulate cortex, lateral temporal cortex, and visual cortex were significant in models for females (Fig. 6f).

Discussion

Female sex is a significant risk factor for insomnia and plays a role in diagnostic heterogeneity, yet the neurobiological mechanisms behind this remain unclear. Our study advances the understanding of CID's neurobiological mechanisms in three main aspects. Firstly, our findings reveal that CID is associated with sex-specific

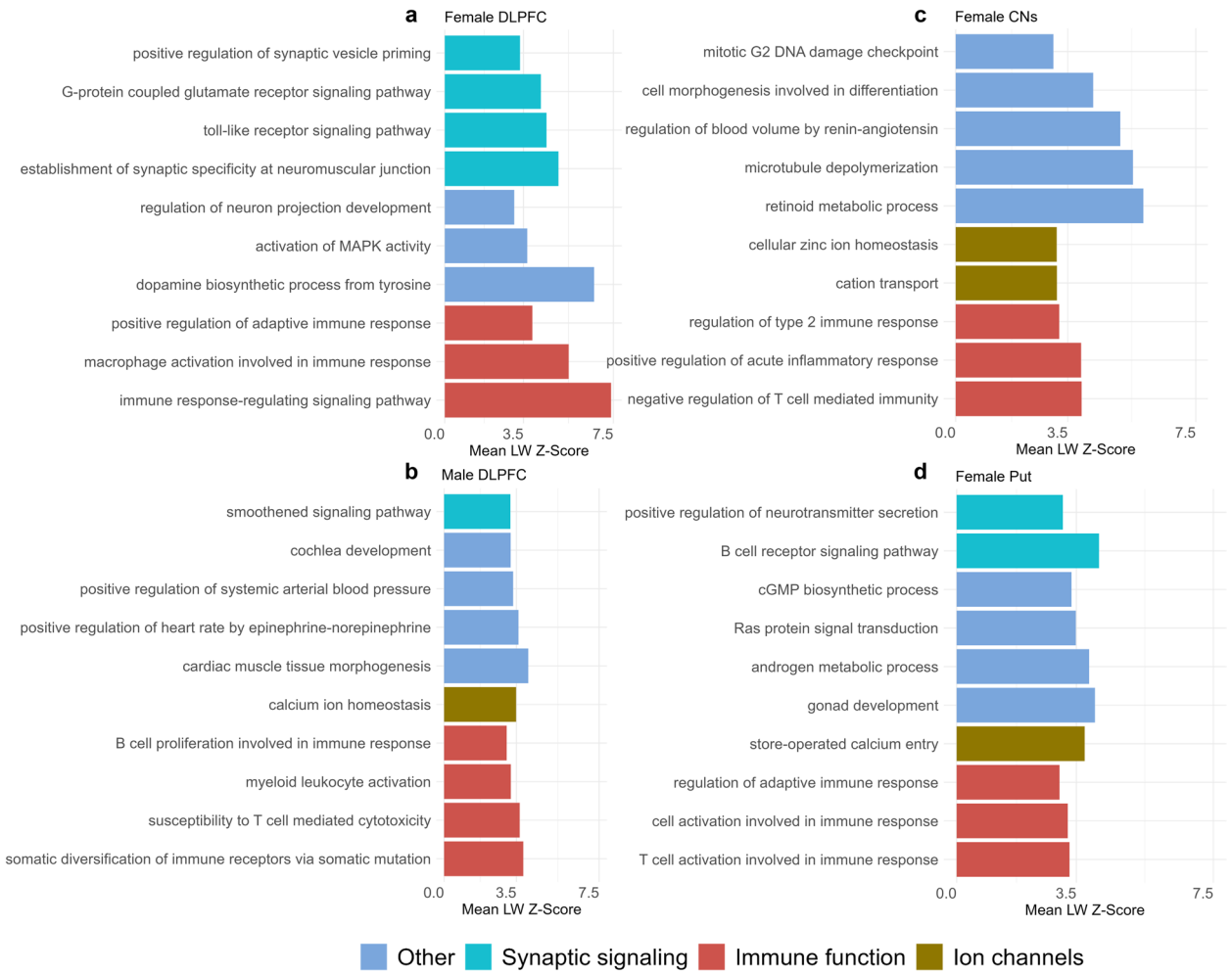

Fig. 5 Functional enrichment of PLS1 weighted genes related to sex-dependent rsFC effects. Top 10 significantly biological terms of PLS1 + (*Z*-score > 3, $p_{FDR} < 0.05$) gene enrichment in four significant and reproducible models: female DLPFC (**a**), male DLPFC (**b**), female CNs (**c**), and female Put (**d**). Statistical significance for each term was evaluated compared to shuffled predictor data ("spin" test, $p_{spin} < 0.05$, see Methods). The mean loading weight *Z*-score for an enriched category was calculated as the mean gene loading weight within the category. The top 10 biological terms of PLS1- (*Z*-score < − 3, $p_{FDR} < 0.05$) gene are presented in Fig. S5. Abbreviations: LW, loading weight; BA, Brodmann area; NAc, nucleus accumbens; CNs, caudate nucleus; Put, putamen

differences in connectivity within the DMN and five ROIs known for their genetic vulnerability to insomnia, which also serve as potential targets for therapy. Secondly, our findings highlight that specific genes related to synaptic transmission, ion channels, and immune signaling could underlie the disorder's pathophysiology by altering connectivity in specific ROIs. Thirdly, our findings demonstrate that sex differences in rsFC are both statistically significant and biologically impactful, as shown by varied outcomes based on different sex compositions and improved diagnostic performance with sex-specific connectivity data. Collectively, these insights uncover shared and sex-specific alterations in functional networks related to CID, offering a molecular basis for understanding the pathophysiology and guiding fMRI-based diagnostics and therapeutic approaches.

DMN hypoconnectivity, often found in rsfMRI studies of insomnia [7, 25, 26, 64], but not all [28, 29], emerges as a potential target for neurostimulation [22, 65], yet sex differences in rsFC have historically been overlooked. Our whole-brain analysis of rsFC within the DMN and its interactions with other networks in CID patients revealed that DMN hypoconnectivity predominantly occurs in men, affecting key areas like the posterior cingulate and ventromedial prefrontal cortex. In contrast, women with CID showed increased rsFC in non-DMN regions, such as the superior parietal, medial cingulate, and visual cortex. It is important to note that the observed variations in connectivity between males and females with CID were not attributable to differences in symptom severity, as both sexes exhibited comparable levels of clinical symptoms. This suggests that the distinct connectivity patterns identified may reflect different underlying mechanisms of CID in males and females, with decreased connectivity being more prevalent in male patients and increased connectivity being more prevalent in female patients [66]. Our findings highlight sex-specific connectivity patterns in insomnia disorders, suggesting fundamental differences in the pathophysiological mechanisms of CID between men and women.

Genome-wide association studies [6, 31, 41] have unveiled over 202 genetic variants linked to 956 genes that increase the risk of insomnia, though their interactive effects on the disorder's pathophysiology remain to be fully understood. Emerging evidence suggests that genetic variations and regional gene expression differences can significantly impact the organization of functional networks [33, 67]. This research specifically explored five areas known for genetic vulnerability in the insomnia study [41]: the dorsolateral prefrontal cortex, anterior cingulate cortex, nucleus accumbens, caudate nucleus, and putamen, which have not been previously analyzed for sex-specific effects. Our analysis indicated distinct connectivity patterns between sexes, with men typically experiencing hypoconnectivity and women hyperconnectivity within these regions. In the dorsolateral prefrontal cortex, men with CID showed reduced connectivity to several brain areas, including the medial prefrontal, temporal pole, and medial cingulate cortex—effects that were conspicuously absent in women. Additionally, in other ROIs such as the nucleus accumbens, anterior cingulate cortex, caudate nucleus, and putamen, the majority of observed effects were also sex-specific, with only a minor percentage (5.5–8.0%) shared between men and women.

These genetically vulnerable regions are not only crucial for understanding insomnia's neuroanatomy but also represent key targets for treatment modalities like transcranial electric stimulation and repetitive transcranial magnetic stimulation (rTMS), which have shown efficacy in symptom management [68, 69]. For instance, the dorsolateral prefrontal cortex is a key site for TMS techniques that have shown promise in modulating neural hyperexcitability and alleviating symptoms of insomnia. Similarly, the anterior cingulate cortex, with its role in emotional processing and regulation, has been targeted in TMS treatments for mood disorders [70, 71], which often co-occur with insomnia [72], suggesting its potential utility in insomnia treatment as well. Moreover, the nucleus accumbens and caudate nucleus, integral to the brain's reward system, have been explored as deep brain stimulation targets for treating addictive behaviors [73, 74], which share neural pathways with insomnia [75], indicating their relevance in insomnia therapies.

(See figure on next page.)

Fig. 6 Sex-specific rsFC effects on biomarker development. **a** Boxplots display the distribution of mean *t*-statistics for rsFC effects associated with the DMN's 83 nodes, analyzed over 1000 bootstrapped samples for seven distinct sex compositions. **b** A color map details the neuroanatomical distribution of rsFC effects, as summarized in **a**. Significant *t*-statistics ($p_{FDR} < 0.05$) are averaged across 83 DMN nodes, with warmer colors denoting significant increases in connectivity. **c** A schematic outlines the 2:1 hold-out approach used for the training and evaluation of EN-GLMs across different groups: males only, females only, and combined sexes. **d, e** Graphs display the AUC for EN-GLMs tested and trained on the combined sample (black lines) and compare performance when models are specific to males (**d**, blue line) or females (**e**, red line). **f** Color maps present the average absolute loading weights for connectivity features associated with each of the 360 cortical ROIs, based on 100 iterations of EN-GLMs. The maps are split to show results from models trained on males only (left), females only (center), and without sex differentiation (right). Abbreviations: F, female; EN-GLMs, Elastic-net regularized general linear models; AUC, area under the receiver operating characteristic curve

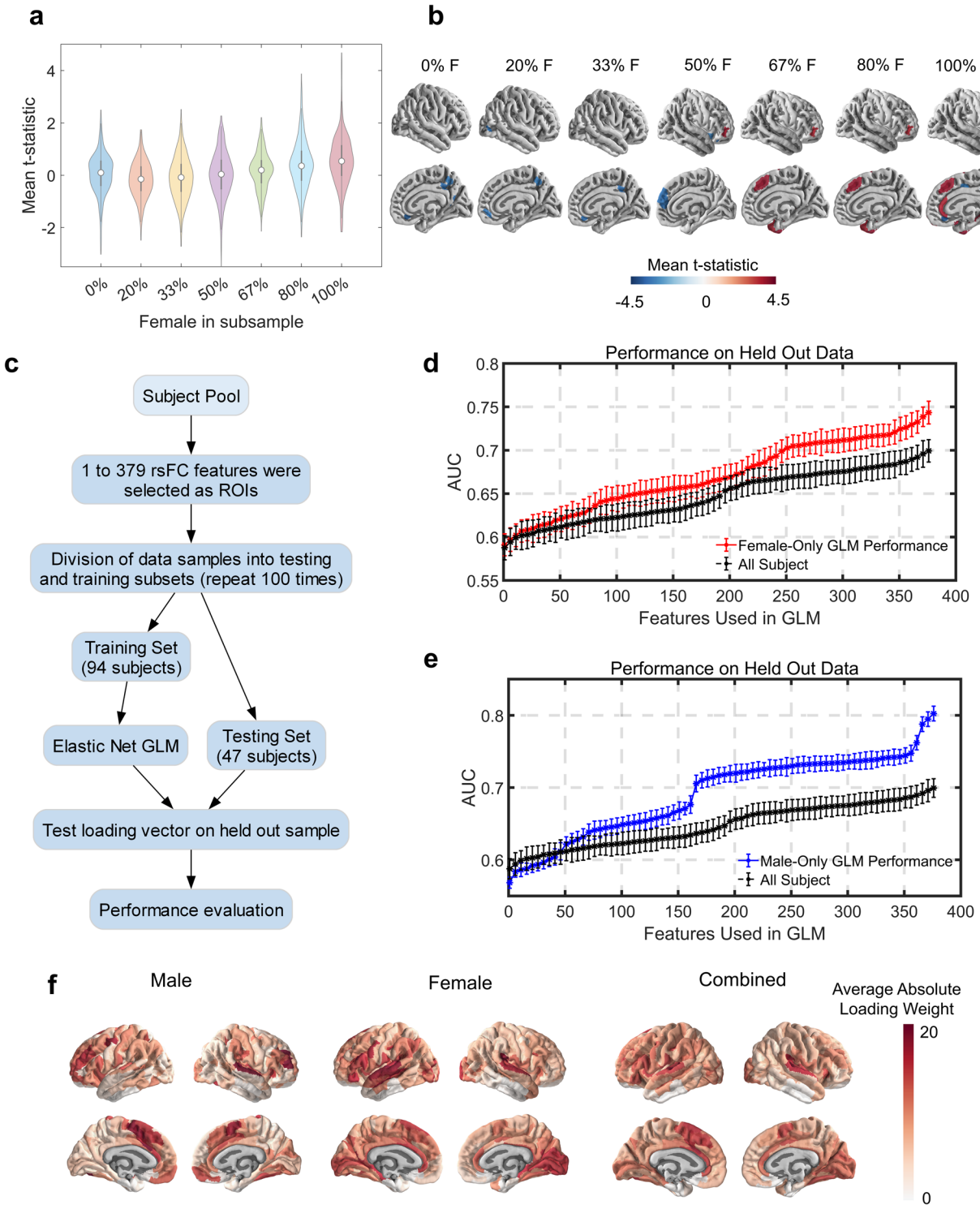

Fig. 6 (See legend on previous page.)

However, to our knowledge, limited studies have considered sex-specific therapeutic strategies, despite the clear evidence of distinct, sometimes opposing, connectivity patterns in the above ROIs between men and women with CID. Our results highlight the need to incorporate sex as a fundamental factor in both research and therapeutic approaches.

In the above five examined regions, CID led to specific alterations in connectivity patterns, which varied between men and women. We proposed that these rsFC differences might be explained by regional variations in gene expression. To investigate this, we aligned normative gene expression data from the Allen Human Brain Atlas [42] with the Glasser functional parcellation [49]. Our methodology aimed to identify genes with significant regional expression (Z-score > 3 or < − 3, $p_{FDR} < 0.05$) [37, 60] that could account for the observed connectivity variations in CID without focusing on sex-biased expression due to limitations in the AHBA data. Our findings indicated that unique gene sets across these regions account for the distinct connectivity patterns seen in CID among males and females. Notably, significantly robust and reproducible associations were found in rsFC changes linked to specific ROIs in the dorsolateral prefrontal cortex, putamen, and caudate nucleus for women and in the dorsolateral prefrontal cortex for men. Aligned with our predictions, the identified gene sets demonstrated variations across both brain regions and sexes. For example, in women, certain genes are positively correlated with connectivity in both the caudate nucleus and putamen but negatively correlated with the DLPFC region, showcasing sex-specific genetic contributions to connectivity differences. Furthermore, we found these gene sets to be significantly associated with synaptic function, ion channels, and immune signaling, aligning with insights from previous GWAS studies [6, 76, 77] on insomnia and other psychiatric conditions [35, 36, 78]. Those findings bridge the understanding between rsFC alterations and their molecular underpinnings in CID.

Additionally, three genes (ZDHHC2, VAT1L, and CHST1) were found as shared genes for rsFC changes associated with CID across sex and 3 ROIs. These genes are involved in key biological processes such as protein modification [79], vesicle transport [80], and intercellular signaling regulation [81], all of which are critical for maintaining normal brain function. For instance, ZDHHC2 plays a role in protein palmitoylation, a modification essential for the membrane localization of neurotransmitter receptors and synaptic proteins [79]. Since the proper transmission of neurotransmitter signals is crucial for maintaining the sleep–wake balance [82], dysfunction in ZDHHC2 could indirectly impair neuronal signaling and the functional connectivity between brain regions. Given that insomnia is a complex sleep disorder influenced by factors such as neurotransmitter regulation [83], neuronal plasticity [84], and neuroendocrine processes [85], abnormalities in these shared genes may contribute to altered sleep quality and patterns. Moreover, our results revealed that the GWAS gene list [41] and the gene lists from our PLS models share additional GO biological processes, particularly those related to brain development and behavior. Those findings underscore the complex genetic basis of insomnia.

Together, our above findings highlight significant sex-specific rsFC deviations in the DMN and in five genetically vulnerable ROIs, as well as decoding connectivity changes from the molecular perspective. To assess how these observed sex differences impact future research, we conducted two key analyses. Firstly, in response to the variability seen in previous rsfMRI studies of insomnia due to different sex compositions, we investigated the effect of sex differences in rsFC, particularly focusing on DMN connectivity. Our analysis demonstrated that samples with a higher proportion of females showed a notable increase in DMN hyperconnectivity, indicating that such sex differences are not merely observable but have substantial biological relevance, potentially accounting for variations seen in earlier studies [16, 39]. Secondly, amid growing interest in refining fMRI biomarkers for accurately diagnosing insomnia subtypes and guiding treatment [15, 86], we utilized elastic-net regularized general linear models to discern insomnia status based on rsFC, analyzing both sex-segregated and combined connectivity data. The sex-specific models outperformed the mixed-sex models in AUC and identified unique connectivity patterns predictive of CID. This provides evidence that sex-based differences in rsFC are predictive of insomnia status and carry enough weight to significantly enhance diagnostic performance, underscoring their importance in future diagnostic frameworks.

Several limitations exist in our study. First, rsFC is influenced by various factors, such as physiological differences [87], neurobiological changes in synaptic connectivity [88], and some psychosocial factors [89]. Our data do not determine whether the observed sex differences are primarily due to biological, psychosocial, or a mix of both. Second, it is crucial to acknowledge that DMN connectivity issues are not exclusive to insomnia. DMN dysfunction varies across numerous neuropsychiatric disorders, such as Alzheimer's disease [90], autism [18], and schizophrenia [91]. Future research is essential to ascertain whether our CID-related findings are unique and if similar mechanisms at the molecular and network levels influence other neuropsychiatric conditions. Third, while the Allen Human Brain Atlas [42] offers insights into the molecular foundations of neuroimaging outcomes, as evidenced by its broad application in previous research [36, 37, 92, 93], its limitations stem from its dependence on brain tissue samples from a limited group of six donors (comprising five men and one predominantly middle-aged woman). This sample size restricts the representation of individual

variability in cortical gene expression and hampers the inclusion of sex differences in gene expression within our PLS regression models. Fourth, our study did not include age as a covariate in the ANOVA, as age differences between the groups were minimal and not statistically significant. Future studies may consider age as a covariate to further validate the robustness of our findings, especially regarding potential age-related effects. Fifth, given that DMN dysfunction is common in many neuropsychiatric diseases, our study did not include direct comparisons with other conditions. Future cross-diagnostic studies with harmonized neuroimaging and omics datasets are critical to disentangle shared versus disorder-specific mechanisms. Finally, PLS regression models inherently establish correlations, not causations, between gene expression and connectivity changes. Yet, they are emerging as powerful tools in systems neuroscience [94–96], enabling the inference of complex associations between macroscopic neuroimaging phenotypes and microscopic gene, cellular, and neurotransmitter expression patterns in the cortex. These models facilitate the development of testable hypotheses on potential mechanisms for future empirical validation.

Conclusions

Our study identified significant rsFC changes within the DMN and five ROIs between men and women, highlighting the potential of genetically vulnerable ROIs in sex-based therapeutic interventions. Furthermore, by utilizing neuroimaging and gene expression data, our results suggest that genes associated with synaptic transmission, ion channels, and immune signaling could influence the pathophysiology by affecting functional connectivity in specific ROIs. Additionally, our analysis confirms that sex differences in rsFC are not only statistically significant but also biologically meaningful, as evidenced by varied outcomes across sex compositions and improved diagnostic accuracy with sex-specific connectivity data. These findings uncover both common and sex-specific alterations in CID-related functional networks, informing potential biomarkers and guiding fMRI-based therapeutic strategies.

Abbreviations

ACC	Anterior cingulate cortex
AHBA	Allen Human Brain Atlas
ANOVA	Analysis of variance
AUC	Area under the receiver operating characteristic curve
BA	Brodmann area
CID	Chronic insomnia disorder
CNs	Caudate nucleus
DLPFC	Dorsolateral prefrontal cortex
DMN	Default mode network
EN-GLMs	Elastic-net regularized general linear models
FD	Framewise displacement
FDR	False discovery rate
HCs	Healthy controls
NAc	Nucleus accumbens
PLS-R	Partial least squares regression
ROIs	Regions of interest
rsFC	Resting-state functional connectivity
rsfMRI	Resting-state functional magnetic resonance imaging
rTMS	Repetitive transcranial magnetic stimulation

Supplementary Information

The online version contains supplementary material available at https://doi.org/10.1186/s12916-025-04089-9.

Supplementary Material 1. Additional File 1. Methods S1: Inclusion and exclusion criteria. Methods S2: Preprocessing of MRI data. Fig. S1: Shared and sex-specific rsFC effects associated with the DMN. Fig. S2: rsFC effects within the DMN between healthy females and males. Fig. S3: Sex-specific rsFC effects at five genetically vulnerable ROIs. Fig. S4: Gene-neuroimaging partial least squares regression score correlations. Fig. S5: Functional enrichment of PLS1 weighted genes related to sex-dependent rsFC effects. Fig. S6: Overlapped genes related to sex-dependent rsFC effects in four significant PLS-R models. Fig. S7: Overlapped Go biological processes terms among PLS1 +, PLS1-, and GWAS study in four PLS-R models. Table S1: The list of the reordered cortical regions of the Glasser atlas. Table S2: List of brain regions exhibiting significant sex-specific effects in males with CID compared to male healthy controls. Table S3: List of brain regions exhibiting significant sex-specific effects in females with CID compared to female healthy controls.

Acknowledgements

We would like to acknowledge all participants in this study.

Authors' contributions

SY and LY were responsible for the conceptualization and design of the study. WW, ZD, YL, DH, WL, and GZ contributed to the collection of the data. SY, LY, and ZS analyzed and interpreted the data. SY and ZS provided critical scientific input. SY and XH supervised the project. All the authors contributed to the writing of the manuscript and read and approved the final version.

Funding

This work was supported by the National Natural Science Foundation of China (No.82374590, No.82305415, and No.82004488), and the Chengdu University of Traditional Chinese Medicine Xinglin Scholar Discipline Talent Research and Improvement Plan (No. QJRC2022036).

Data availability

The original MRI data that support the findings of this study are available on request from the corresponding author. Data supporting the study's findings on human gene expression can be found in the Allen Human Brain Atlas database, accessible at http://human.brain-map.org/static/download.

Declarations

Ethics approval and consent to participate

The study received approval from the Ethics Committees of the Affiliated Hospital of Chengdu University of Traditional Chinese Medicine, and all participants provided written informed consent prior to their participation.

Consent for publication

Not applicable.

Competing interests

The authors declare no competing interests.

Author details

[1]School of Acupuncture and Tuina, Chengdu University of Traditional Chinese Medicine, No.37 Shierqiao Road, Chengdu 610075, China. [2]Department of Traditional Chinese Medicine, the Affiliated Hospital of North Sichuan Medical

College, Nanchong, China. [3]Department of Traditional Chinese and Western Medicine, North Sichuan Medical College, Nanchong, China. [4]School of Rehabilitation and Health Preservation, Chengdu University of Traditional Chinese Medicine, Chengdu, China.

Received: 2 April 2024 Accepted: 24 April 2025
Published: 6 May 2025

References

1. Zhang B, Wing Y-K. Sex Differences in Insomnia: A Meta-Analysis. Sleep. 2006;29:85–93.
2. Swaab DF, Van Someren EJW, Zhou JN, Hofman MA. Biological rhythms in the human life cycle and their relationship to functional changes in the suprachiasmatic nucleus. Prog Brain Res. 1996;111:349–68.
3. Bangasser DA, Wiersielis KR, Khantsis S. Sex differences in the locus coeruleus-norepinephrine system and its regulation by stress. Brain Res. 2016;1641 PtB:177–88.
4. Nielsen TA, Laberge L, Paquet J, Tremblay RE, Vitaro F, Montplaisir J. Development of disturbing dreams during adolescence and their relation to anxiety symptoms. Sleep. 2000;23:727–36.
5. Yuksel D, Kiss O, Prouty DE, Baker FC, De Zambotti M. Clinical characterization of insomnia in adolescents - an integrated approach to psychopathology. Sleep Med. 2022;93:26–38.
6. Lane JM, Liang J, Vlasac I, Anderson SG, Bechtold DA, Bowden J, et al. Genome-wide association analyses of sleep disturbance traits identify new loci and highlight shared genetics with neuropsychiatric and metabolic traits. Nat Genet. 2017;49:274–81.
7. Shen Z, Yang X, She T, Zhao G, Dou Z, Luo Y, et al. Deficits in brain default mode network connectivity mediate the relationship between poor sleep quality and anxiety severity. Sleep. 2024;47:zsad296.
8. Wassing R, Schalkwijk F, Lakbila-Kamal O, Ramautar JR, Stoffers D, Mutsaerts HJMM, et al. Haunted by the past: old emotions remain salient in insomnia disorder. Brain J Neurol. 2019;142:1783–96.
9. Altena E, Van Der Werf YD, Sanz-Arigita EJ, Voorn TA, Rombouts SARB, Kuijer JPA, et al. Prefrontal hypoactivation and recovery in insomnia. Sleep. 2008;31:1271–6.
10. Jiang G, Li C, Ma X, Dong M, Yin Y, Hua K, et al. Abnormal spontaneous regional brain activity in primary insomnia: a resting-state functional magnetic resonance imaging study. Neuropsychiatr Dis Treat. 2016;12:1371-8.
11. Stoffers D, Altena E, Van Der Werf YD, Sanz-Arigita EJ, Voorn TA, Astill RG, et al. The caudate: a key node in the neuronal network imbalance of insomnia? Brain. 2014;137:610–20.
12. Chen T, Cai W, Ryali S, Supekar K, Menon V. Distinct Global Brain Dynamics and Spatiotemporal Organization of the Salience Network. PLOS Biol. 2016;14: e1002469.
13. Drummond SPA, Walker M, Almklov E, Campos M, Anderson DE, Straus LD. Neural correlates of working memory performance in primary insomnia. Sleep. 2013;36:1307–16.
14. Lee Y-JG, Kim S, Kim N, Choi J, Park J-W, Kim SJ, et al. Changes in subcortical resting-state functional connectivity in patients with psychophysiological insomnia after cognitive-behavioral therapy: Changes in resting-state FC after CBT for insomnia patients. Neuro Image Clin. 2018;17:115–23.
15. Zheng H, Zhou Q, Yang J, Lu Q, Qiu H, He C, et al. Altered functional connectivity of the default mode and frontal control networks in patients with insomnia. CNS Neurosci Ther. 2023;29:2318–26.
16. Fasiello E, Gorgoni M, Scarpelli S, Alfonsi V, Ferini Strambi L, De Gennaro L. Functional connectivity changes in insomnia disorder: A systematic review. Sleep Med Rev. 2022;61: 101569.
17. Marques DR, Gomes AA, Caetano G, Castelo-Branco M. Insomnia Disorder and Brain's Default-Mode Network. Curr Neurol Neurosci Rep. 2018;18:45.
18. Curtin P, Neufeld J, Curtin A, Arora M, Bölte S. Altered Periodic Dynamics in the Default Mode Network in Autism and Attention-Deficit/Hyperactivity Disorder. Biol Psychiatry. 2022;91:956–66.
19. Guàrdia-Olmos J, Soriano-Mas C, Tormo-Rodríguez L, Cañete-Massé C, Cerro ID, Urretavizcaya M, et al. Abnormalities in the default mode network in late-life depression: A study of resting-state fMRI. Int J Clin Health Psychol. 2022;22: 100317.
20. Fan F, Tan S, Huang J, Chen S, Fan H, Wang Z, et al. Functional disconnection between subsystems of the default mode network in schizophrenia. Psychol Med. 2022;52:2270–80.
21. Han S, Gao J, Hu J, Ye Y, Huang H, Liu J, et al. Disruptions of salience network during uncertain anticipation of conflict control in anxiety. Asian J Psychiatry. 2023;88: 103721.
22. Liston C, Chen AC, Zebley BD, Drysdale AT, Gordon R, Leuchter B, et al. Default mode network mechanisms of transcranial magnetic stimulation in depression. Biol Psychiatry. 2014;76:517–26.
23. Fang J, Rong P, Hong Y, Fan Y, Liu J, Wang H, et al. Transcutaneous Vagus Nerve Stimulation Modulates Default Mode Network in Major Depressive Disorder. Biol Psychiatry. 2016;79:266–73.
24. Li C, Dong M, Yin Y, Hua K, Fu S, Jiang G. Aberrant Effective Connectivity of the Right Anterior Insula in Primary Insomnia. Front Neurol. 2018;9:317.
25. Gong L, Yu S, Xu R, Liu D, Dai X, Wang Z, et al. The abnormal reward network associated with insomnia severity and depression in chronic insomnia disorder. Brain Imaging Behav. 2021;15:1033–42.
26. Park HY, Lee H, Jhee JH, Park KM, Choi EC, An SK, et al. Changes in resting-state brain connectivity following computerized cognitive behavioral therapy for insomnia in dialysis patients: A pilot study. Gen Hosp Psychiatry. 2020;66:24–9.
27. Wang T, Ye Y, Li S, Jiang G. Altered functional connectivity of anterior cingulate cortex in chronic insomnia: A resting-state fMRI study. Sleep Med. 2023;102:46–51.
28. Yu S, Guo B, Shen Z, Wang Z, Kui Y, Hu Y, et al. The imbalanced anterior and posterior default mode network in the primary insomnia. J Psychiatr Res. 2018;103:97–103.
29. Li C, Liu Y, Yang N, Lan Z, Huang S, Wu Y, et al. Functional Connectivity Disturbances of the Locus Coeruleus in Chronic Insomnia Disorder. Nat Sci Sleep. 2022;14:1341–50.
30. Dai X-J, Nie X, Liu X, Pei L, Jiang J, Peng D, et al. Gender Differences in Regional Brain Activity in Patients with Chronic Primary Insomnia: Evidence from a Resting-State fMRI Study. J Clin Sleep Med. 2016;12:363–74.
31. Byrne EM. The relationship between insomnia and complex diseases—insights from genetic data. Genome Med. 2019;11:57.
32. Xiang B, Liu K, Yu M, Liang X, Huang C, Zhang J, et al. Systematic genetic analyses of GWAS data reveal an association between the immune system and insomnia. Mol Genet Genomic Med. 2019;7: e00742.
33. Váša F, Romero-Garcia R, Kitzbichler MG, Seidlitz J, Whitaker KJ, Vaghi MM, et al. Conservative and disruptive modes of adolescent change in human brain functional connectivity. Proc Natl Acad Sci U S A. 2020;117:3248–53.
34. Richiardi J, Altmann A, Milazzo A-C, Chang C, Chakravarty MM, Banaschewski T, et al. Correlated gene expression supports synchronous activity in brain networks. Science. 2015;348:1241–4.
35. Li J, Seidlitz J, Suckling J, Fan F, Ji G-J, Meng Y, et al. Cortical structural differences in major depressive disorder correlate with cell type-specific transcriptional signatures. Nat Commun. 2021;12:1647.
36. Talishinsky A, Downar J, Vértes PE, Seidlitz J, Dunlop K, Lynch CJ, et al. Regional gene expression signatures are associated with sex-specific functional connectivity changes in depression. Nat Commun. 2022;13:5692.
37. Morgan SE, Seidlitz J, Whitaker KJ, Romero-Garcia R, Clifton NE, Scarpazza C, et al. Cortical patterning of abnormal morphometric similarity in psychosis is associated with brain expression of schizophrenia-related genes. Proc Natl Acad Sci. 2019;116:9604–9.
38. Luo Y, Dong D, Huang H, Zhou J, Zuo X, Hu J, et al. Associating Multimodal Neuroimaging Abnormalities With the Transcriptome and Neurotransmitter Signatures in Schizophrenia. Schizophr Bull. 2023;49:1554–67.
39. Van Someren EJW. Brain mechanisms of insomnia: new perspectives on causes and consequences. Physiol Rev. 2021;101:995–1046.
40. Khazaie H, Veronese M, Noori K, Emamian F, Zarei M, Ashkan K, et al. Functional reorganization in obstructive sleep apnoea and insomnia: A systematic review of the resting-state fMRI. Neurosci Biobehav Rev. 2017;77:219–31.
41. The 23andMe Research Team, Jansen PR, Watanabe K, Stringer S, Skene N, Bryois J, et al. Genome-wide Analysis of Insomnia (N=1,331,010) Identifies Novel Loci and Functional Pathways. Nat Genet. 2019;51:394–403.
42. Hawrylycz MJ, Lein ES, Guillozet-Bongaarts AL, Shen EH, Ng L, Miller JA, et al. An anatomically comprehensive atlas of the adult human brain transcriptome. Nature. 2012;489:391–9.

43. Sateia MJ. International classification of sleep disorders-third edition: highlights and modifications. Chest. 2014;146:1387–94.
44. Liu X. Reliability and validity of the Pittsburgh sleep quality index. Chin J Psychiatry. 1996;29:103.
45. Esteban O, Markiewicz CJ, Blair RW, Moodie CA, Isik AI, Erramuzpe A, et al. fMRIPrep: a robust preprocessing pipeline for functional MRI. Nat Methods. 2019;16:111–6.
46. Ciric R, Wolf DH, Power JD, Roalf DR, Baum GL, Ruparel K, et al. Benchmarking of participant-level confound regression strategies for the control of motion artifact in studies of functional connectivity. Neuroimage. 2017;154:174–87.
47. Ciric R, Rosen AFG, Erus G, Cieslak M, Adebimpe A, Cook PA, et al. Mitigating head motion artifact in functional connectivity MRI. Nat Protoc. 2018;13:2801–26.
48. Satterthwaite TD, Elliott MA, Gerraty RT, Ruparel K, Loughead J, Calkins ME, et al. An improved framework for confound regression and filtering for control of motion artifact in the preprocessing of resting-state functional connectivity data. Neuroimage. 2013;64:240–56.
49. Schaefer A, Kong R, Gordon EM, Laumann TO, Zuo X-N, Holmes AJ, et al. Local-Global Parcellation of the Human Cerebral Cortex from Intrinsic Functional Connectivity MRI. Cereb Cortex. 2018;28:3095–114.
50. Pauli WM, Nili AN, Tyszka JM. A high-resolution probabilistic in vivo atlas of human subcortical brain nuclei. Sci Data. 2018;5: 180063.
51. Avants BB, Tustison NJ, Song G, Cook PA, Klein A, Gee JC. A reproducible evaluation of ANTs similarity metric performance in brain image registration. Neuroimage. 2011;54:2033–44.
52. Fischl B. FreeSurfer NeuroImage. 2012;62:774–81.
53. Thomas Yeo BT, Krienen FM, Sepulcre J, Sabuncu MR, Lashkari D, Hollinshead M, et al. The organization of the human cerebral cortex estimated by intrinsic functional connectivity. J Neurophysiol. 2011;106:1125–65.
54. Paquola C, De Vos Wael R, Wagstyl K, Bethlehem RAI, Hong S-J, Seidlitz J, et al. Microstructural and functional gradients are increasingly dissociated in transmodal cortices. PLOS Biol. 2019;17:3000284.
55. Krishnan A, Williams LJ, McIntosh AR, Abdi H. Partial Least Squares (PLS) methods for neuroimaging: a tutorial and review. Neuroimage. 2011;56:455–75.
56. Fulcher BD, Arnatkeviciute A, Fornito A. Overcoming false-positive gene-category enrichment in the analysis of spatially resolved transcriptomic brain atlas data. Nat Commun. 2021;12:2669.
57. Markello RD, Arnatkeviciute A, Poline JB, Fulcher BD, Fornito A, Misic B. Standardizing workflows in imaging transcriptomics with the abagen toolbox. ELife. 2021;10:72129.
58. Váša F, Seidlitz J, Romero-Garcia R, Whitaker KJ, Rosenthal G, Vértes PE, et al. Adolescent Tuning of Association Cortex in Human Structural Brain Networks. Cereb Cortex. 2018;28:281–94.
59. Nadeau C. Inference for the Generalization Error. Mach Learn. 2003;52:239–81.
60. Martins D, Dipasquale O, Veronese M, Turkheimer F, Loggia ML, McMahon S, et al. Transcriptional and cellular signatures of cortical morphometric remodelling in chronic pain. Pain. 2022;163:e759–73.
61. Zhou Y, Zhou B, Pache L, Chang M, Khodabakhshi AH, Tanaseichuk O, et al. Metascape provides a biologist-oriented resource for the analysis of systems-level datasets. Nat Commun. 2019;10:1523.
62. Yang L, Yu S, Zhang L, Peng W, Hu Y, Feng F, et al. Gender differences in hippocampal/parahippocampal functional connectivity network in patients diagnosed with chronic insomnia disorder. Nat Sci Sleep. 2022;14:1175–86.
63. Zhao W, Van Someren EJW, Li C, Chen X, Gui W, Tian Y, et al. EEG spectral analysis in insomnia disorder: A systematic review and meta-analysis. Sleep Med Rev. 2021;59: 101457.
64. Gong L, Chen K, Zhang H, Zhang S, Xu R, Liu D, et al. Dopamine multilocus genetic profile influence on reward network in chronic insomnia disorder with depression. Sleep Med. 2023;112:122–8.
65. Webler RD, Fox J, McTeague LM, Burton PC, Dowdle L, Short EB, et al. DLPFC stimulation alters working memory related activations and performance: An interleaved TMS-fMRI study. Brain Stimulat. 2022;15:823–32.
66. Yuan C, Jian Z, Jin X. Chronotype and insomnia may affect the testosterone levels with a sexual difference: a Mendelian randomization. J Endocrinol Invest. 2022;46:123–32.
67. Martins D, Dipasquale O, Davies K, Cooper E, Tibble J, Veronese M, et al. Transcriptomic and cellular decoding of functional brain connectivity changes reveal regional brain vulnerability to pro- and anti-inflammatory therapies. Brain Behav Immun. 2022;102:312–23.
68. Krone LB, Fehér KD, Rivero T, Omlin X. Brain stimulation techniques as novel treatment options for insomnia: A systematic review. J Sleep Res. 2023;32: e13927.
69. Lanza G, Fisicaro F, Cantone M, Pennisi M, Cosentino FII, Lanuzza B, et al. Repetitive transcranial magnetic stimulation in primary sleep disorders. Sleep Med Rev. 2023;67: 101735.
70. Galhardoni R, Da Aparecida Silva V, García-Larrea L, Dale C, Baptista AF, Barbosa LM, et al. Insular and anterior cingulate cortex deep stimulation for central neuropathic pain: Disassembling the percept of pain. Neurology. 2019;92:2165–75.
71. Iseger TA, Van Bueren NER, Kenemans JL, Gevirtz R, Arns M. A frontal-vagal network theory for Major Depressive Disorder: Implications for optimizing neuromodulation techniques. Brain Stimulat. 2020;13:1–9.
72. Zhao G, Yu L, Chen P, Zhu K, Yang L, Lin W, et al. Neural mechanisms of attentional bias to emotional faces in patients with chronic insomnia disorder. J Psychiatr Res. 2024;169:49–57.
73. Ho AL, Salib A-MN, Pendharkar AV, Sussman ES, Giardino WJ, Halpern CH. The nucleus accumbens and alcoholism: a target for deep brain stimulation. Neurosurg Focus. 2018;45:E12.
74. Aouizerate B, Cuny E, Martin-Guehl C, Guehl D, Amieva H, Benazzouz A, et al. Deep brain stimulation of the ventral caudate nucleus in the treatment of obsessive-compulsive disorder and major depression. Case report J Neurosurg. 2004;101:682–6.
75. Ling J, Lin X, Li X, Chan NY, Zhang J, Wing YK, et al. Neural response to rewards in youths with insomnia. Sleep. 2022;45:zsab238.
76. Lin Y-S, Wang C-C, Chen C-Y. GWAS Meta-Analysis Reveals Shared Genes and Biological Pathways between Major Depressive Disorder and Insomnia. Genes. 2021;12:1506.
77. Ding M, Li P, Wen Y, Zhao Y, Cheng B, Zhang L, et al. Integrative analysis of genome-wide association study and brain region related enhancer maps identifies biological pathways for insomnia. Prog Neuropsychopharmacol Biol Psychiatry. 2018;86:180–5.
78. Yu L, Chen X, He Y, Hong X, Yu S. Age-specific functional connectivity changes after partial sleep deprivation are correlated with neurocognitive and molecular signatures. CNS Neurosci Ther. 2025;31: e70272.
79. Ramanan VK, Lesnick TG, Przybelski SA, Heckman MG, Knopman DS, Graff-Radford J, et al. Coping with brain amyloid: genetic heterogeneity and cognitive resilience to alzheimer's pathophysiology. Acta Neuropathol Commun. 2021;9:48.
80. Rushing BR. Multi-omics analysis of NCI-60 cell line data reveals novel metabolic processes linked with resistance to alkylating anti-cancer agents. Int J Mol Sci. 2023;24:13242.
81. Kumagai T, Kiwamoto T, Brummet ME, Wu F, Aoki K, Zhu Z, et al. Airway glycomic and allergic inflammatory consequences resulting from keratan sulfate galactose 6-O-sulfotransferase (CHST1) deficiency. Glycobiology. 2018;28:406–17.
82. Yu L, Peng W, Lin W, Luo Y, Hu D, Zhao G, et al. Electroencephalography connectome changes in chronic insomnia disorder are correlated with neurochemical signatures. Sleep. 2024;47:zsae080.
83. Yu L, Yang L, Xiaoqin C, Zheng X, Dou Z, Xiao X, et al. Cerebral blood flow changes and their spatial correlations with GABAa and dopamine-D1 receptor explaining individual differences in chronic insomnia and the therapeutic effects of acupuncture. Hum Brain Mapp. 2025;46: e70183.
84. Yu L, Hu D, Luo Y, Lin W, Xu H, Xiao X, et al. Transcriptional signatures of cortical structural changes in chronic insomnia disorder. Psychophysiology. 2024;61: e14671.
85. Luo Y, Yu L, Zhang P, Lin W, Xu H, Dou Z, et al. Larger hypothalamic subfield volumes in patients with chronic insomnia disorder and relationships to levels of corticotropin-releasing hormone. J Affect Disord. 2024;351:870–7.
86. Xu H, Dou Z, Luo Y, Yang L, Xiao X, Zhao G, et al. Neuroimaging profiles of the negative affective network predict anxiety severity in patients with chronic insomnia disorder: A machine learning study. J Affect Disord. 2023;340:542–50.
87. Gordon EM, Chauvin RJ, Van AN, Rajesh A, Nielsen A, Newbold DJ, et al. A somato-cognitive action network alternates with effector regions in motor cortex. Nature. 2023;617:351–9.

88. Song X, Chen X, Yuksel C, Yuan J, Pizzagalli DA, Forester B, et al. Bioenergetics and abnormal functional connectivity in psychotic disorders. Mol Psychiatry. 2021;26:2483–92.
89. Tobia MJ, Hayashi K, Ballard G, Gotlib IH, Waugh CE. Dynamic functional connectivity and individual differences in emotions during social stress. Hum Brain Mapp. 2017;38:6185–205.
90. Wei L, Zhang Y, Wang J, Xu L, Yang K, Lv X, et al. Parietal-hippocampal rTMS improves cognitive function in Alzheimer's disease and increases dynamic functional connectivity of default mode network. Psychiatry Res. 2022;315: 114721.
91. King S, Mothersill D, Holleran L, Patlola SR, Burke T, McManus R, et al. Early life stress, low-grade systemic inflammation and weaker suppression of the default mode network (DMN) during face processing in Schizophrenia. Transl Psychiatry. 2023;13:213.
92. Xue K, Guo L, Zhu W, Liang S, Xu Q, Ma L, et al. Transcriptional signatures of the cortical morphometric similarity network gradient in first-episode, treatment-naive major depressive disorder. Neuropsychopharmacology. 2023;48:518–28.
93. Yao G, Zou T, Luo J, Hu S, Yang L, Li J, et al. Cortical structural changes of morphometric similarity network in early-onset schizophrenia correlate with specific transcriptional expression patterns. BMC Med. 2023;21:479.
94. Hansen JY, Markello RD, Vogel JW, Seidlitz J, Bzdok D, Misic B. Mapping gene transcription and neurocognition across human neocortex. Nat Hum Behav. 2021;5:1240–50.
95. Hansen JY, Shafiei G, Markello RD, Smart K, Cox SML, Nørgaard M, et al. Mapping neurotransmitter systems to the structural and functional organization of the human neocortex. Nat Neurosci. 2022;25:1569–81.
96. Martins D, Giacomel A, Williams SCR, Turkheimer F, Dipasquale O, Veronese M. Imaging transcriptomics: Convergent cellular, transcriptomic, and molecular neuroimaging signatures in the healthy adult human brain. Cell Rep. 2021;37: 110173.

Publisher's Note